Numerical investigation of laminar flow in symmetric and asymmetric complex T-channels for micro-mixing

A. Correia[1], A. Afonso[2], A. Cavadas[1], M. S. N. Oliveira[2], M. A. Alves[2] and F. T. Pinho[1]

[1] Departamento de Engenharia Mecânica, CEFT, Faculdade de Engenharia da Universidade do Porto, Rua Dr. Roberto Frias s/n, 4200-465 Porto, Portugal,
email: amrc@fe.up.pt; adelioc@fe.up.pt; fpinho@fe.up.pt
[2] Departamento de Engenharia Química, CEFT, Faculdade de Engenharia da Universidade do Porto, Rua Dr. Roberto Frias s/n, 4200-465 Porto, Portugal, aafonso@fe.up.pt, monica.oliveira@fe.up.pt, mmalves@fe.up.pt

Abstract

A numerical investigation of the flow and mass transfer of Newtonian fluids in two T-micromixers was carried out using a finite volume code. One channel presents a symmetric flow configuration and the other an asymmetric configuration. The Reynolds number was varied between 0.05 and 100 and the Péclet number was varied between 5×10^2 and 5×10^4 for the asymmetric geometry and between 7.5×10^2 and 7.5×10^4 for the symmetric channel. To help assess the mixing efficiency in addition to the analysis of the contours of concentration of a scalar, an index was used to quantify the degree of mixing showing that the asymmetric geometry performed slightly better than the symmetric channel.

Keywords: *Micro-mixing; T-channels; Numerical simulations; Newtonian fluids.*

1 Introduction

The availability since the mid-1990s of cheap manufacturing techniques for micro-fabrication has helped foster investigation and application of micron-sized devices in a variety of systems. A related concept is that of the lab-on-a-chip, which integrates various features to perform a specific task, such as a single or various chemical analysis. In such systems it is usually necessary to transport and mix various fluids, and since this process takes place in small sized devices, the flow is typically laminar in which case mixing occurs slowly by diffusion, unless some other mechanism takes over. Therefore, it is not surprising that the development of cheap and quick micro-manufacturing techniques led to a considerable amount of research in fluid micro-mixing [1,2].
Mixing helped by chaotic advection requires fairly large Reynolds numbers (Re >100), whereas for Re <<1 diffusion completely dominates the flow [3,4] unless other mechanisms are brought into play, as is the case of secondary flows or instabilities induced by elastic forces for non-Newtonian viscoelastic fluid flows. Many studies have been carried out to investigate the mixing performance of the T-shaped micro-channel taking into account the operating principle, i.e. active or passive mixer design. Passive micromixers do not require external energy input for the mixing process itself, which relies on diffusion alone or in combination with strategies, such as chaotic advection [5], turbulence or mechanical agitation. All these increase of mixing efficiency by folding and stretching different pieces of fluid material to increase their interfacial area, decreases the diffusion length and consequently anticipating the final part of the mixing process always occurring by molecular diffusion. As a basic design, the T-shaped channel is ideal for investigations of basic transport phenomena at the microscale, such as scaling laws or the effects of nonlinear forcing or fluid rheology.
In microfluidics, there are inherent difficulties to include mechanical agitation, which severely increases the manufacturing costs of the devices [4]. In addition, the small length scales reduce the Reynolds number (Re) and dampen the role of non-linear phenomena that enhance mixing, often leaving to molecular diffusion the whole task of mixing the different streams. This reduces mixing performance unless the flow rate is reduced to increase transit time and mixing efficiency by diffusion with a corresponding reduction in yield. At moderate and high Re, the fluid inertial effects usually facilitate the chaotic mixing. At low Re, the generation of chaotic advection becomes more difficult, but can be realized by manipulating the laminar flow in microchannels [5]. Full mixing can always be achieved by using sufficiently long channels, but then the corresponding pressure drop increases, pumping becomes expensive and the structural integrity of the micro-channels is threatened. Alternatively the pressure drop can be limited to avoid damage, but then the flow rate will be reduced dramatically and the production rates become too small. Hence, there is a real need for other efficient mechanisms for improved mixing while allowing for high flow rates of the mixed product [3,6] .

A critical dimension that governs the extent of diffusion is the diffusion distance, along which diffusion occurs between adjacent streams. According to the classic diffusion theory, small molecules with a high diffusion coefficient can diffuse significant distances and redistribute between streams on the residence time scale. Diffusion in a T-micromixer can be controlled by adjusting flow conditions and geometry, especially the aspect ratio (height/width), which are used to help fast mixing and chemical reactions [7]. The aspect ratio of mixing channels and the inlet angles are geometrical properties that receive most of the attention in microfluidics design [8]. Besides diffusion, advection is another important mechanism of mass transfer at low Reynolds number flows, and is a key factor for passive mixer design. The simplest method to generate chaotic advection is to insert obstacles in the mixing channel walls. Currently, the T-micromixer is frequently used for generation of concentration gradients and microfluidic diffusion [8], with symmetrical and asymmetrical microstructures embedded in the geometry to improve mixing in compact lab-on-chip and generate a desired concentration gradients. The obstacles in very low Reynolds number flows cannot generate recirculations or eddies, but can improve mixing performance especially as the Reynolds number increases [9].
In this work we perform some preliminary calculations of the flow characteristics of Newtonian fluids in two simple T- mixers and subsequently use the fluid dynamic solutions to calculate mass transfer by diffusion and convection and to qualify the mixing efficiency of the geometries.
The T-micromixers under investigation have two separate inlets and a channel leading to a single outlet, which has a width of the order of one hundred microns and a length of the order of some millimeters. In addition, the walls are not straight, but have some complex shapes, in order to help promote mixing by increasing the contact surface between the different fluids and decreasing the diffusion path between them [6]. The paper is organized as follows: after this initial introduction, the flow geometries are presented in Section 2, the governing equations and a very brief description of the numerical method are given in Section 3. Then, the results of this numerical work are presented and discussed in sequence for each geometry,in section 4. The paper closes with the main conclusions and an outline of future research.

2 Flow geometry

Two basic passive mixer configurations are considered in this preliminary investigation. Both configurations are based on the T-Channel geometry with two entrances and one main exit channel, in which a number of symmetrical or asymmetrical constrictions are combined to create meandering particle trajectories in order to enhance the role of advection forces, increase the contact interfacial area between the two fluid streams and reduce the diffusion distance. The main channel in both geometries has a maximum width of 250µm. The symmetric channel has five successive 3:1:3 contraction-expansions with a total length of 1500µm, part of which is shown in Figure 1a). The asymmetric channel is built around asymmetrical constrictions along the channel length, as illustrated in Figure 1b). The latter geometry has two types of asymmetric obstacles with different disturbance lengths between the upper and lower walls of the microchannel. The first pair of obstacles has a disturbance length of 1/3 of width of the microchannel, whereas the second pair of obstacles has a length of one half the width of the microchannel. The element formed by these two pairs of obstacles is repeated five times along the microchannel, so the total length is 3333µm.

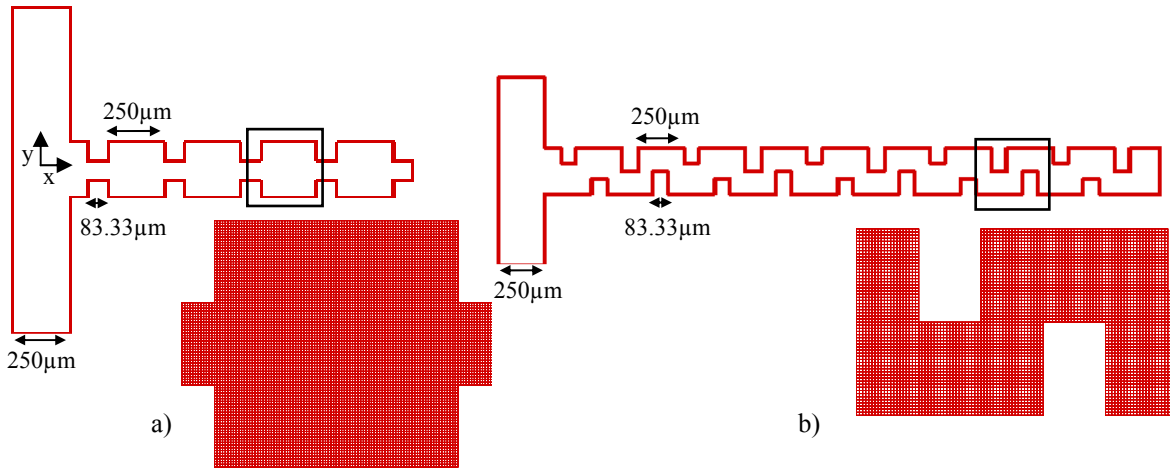

Fig. 1 - Flow domain and mesh for the symmetric geometry (a) and the asymmetric geometry (b). The zoomed views show the mesh in one of the repeating elements.

3 Governing Equations and Numerical Method

The fluid flow behavior in the mixing geometries was studied numerically using an in-house code developed for viscoelastic fluids, even though here the fluids investigated were Newtonian. These calculations provided qualitative flow characteristics, such as flow patterns, as well as quantitative characteristics such as velocity, pressure and stress fields. In addition, once the flow field is know a passive scalar equation can be solved from which a mixing efficiency is quantified.
The numerical method is based on the finite volume methodology and uses three-dimensional collocated non-orthogonal meshes. The code has been extensively validated over the years in a variety of flow conditions and geometries [10] and presents good stability and convergence. Details of the numerical code can be found elsewhere [11, 12]. In this work we focus on the flow of Newtonian fluids through two-dimensional micro-mixers, obeying the Navier-Stokes Eq. (1) and the continuity Eq. (2) for incompressible fluids flowing in a horizontal channel, i.e., without gravitational effects [4].

$$\rho\left(\frac{\partial \mathbf{v}}{\partial t} + \mathbf{v}.\boldsymbol{\nabla}\mathbf{v}\right) = -\boldsymbol{\nabla}p + \mu\boldsymbol{\nabla}^2\mathbf{v} \qquad (1)$$

$$\boldsymbol{\nabla}.\mathbf{v} = 0 \qquad (2)$$

In these equations **v**, t, ρ and μ are the velocity vector, the time, the pressure and the viscosity coefficient, respectively. To investigate mixing performance the convection-diffusion Eq. (3) is solved for the passive scalar c, which represents the mass conservation of a solute [3,4] via its concentration $c(x, y, t)$.

$$\frac{\partial c}{\partial t} + \mathbf{v}.\boldsymbol{\nabla}c = D\boldsymbol{\nabla}^2\mathrm{c} \qquad (3)$$

Here D is the diffusivity coefficient (considered constant). Since the diffusivity coefficient is a constant property, the momentum and continuity equations are decoupled from the scalar problem, and the flow problem can be solved first. Once the flow was known, the code was run to solve the scalar equation using as input the previously calculated flow field. In this way, it becomes quite efficient to test for the effect of the diffusivity coefficient at a constant Reynolds number since only the scalar equation needs to be calculated. This scalar equation was implemented into the finite-volume code and the numerical schemes used to discretize the diffusive and convective fluxes were the second-order central differences scheme and CUBISTA high-resolution scheme of Alves et al [11], respectively. As described by Alves et al [11], the CUBISTA scheme was implemented into the code using the deferred correction approach and it is third order accurate in uniform meshes.
Two important dimensionless numbers govern this mixing problem, namely the Reynolds number (*Re*) and the Péclet number (*Pe*). The Reynolds number represents the ratio between inertial and viscous forces and is defined here as:

$$Re = \frac{\rho v d}{\mu} \qquad (4)$$

where d is a characteristic length scale taken here as the half-width of the channel. When $Re \ll 1$ inertial effects are negligible and the flow is dominated by viscous forces [4]. The Péclet number is defined here as:

$$Pe = \frac{vd}{D} \qquad (5)$$

The Péclet number quantifies the ratio between the mass transport by advection and by molecular diffusion; therefore convection dominates at high Péclet numbers. From Eqs. (4) and (5) it is clear that we can relate the two non-dimensional numbers by $Pe = Re \times \nu/D$, where ν is the molecular diffusivity of momentum. The ratio ν/D is widely known as the Schmidt number and represents the ratio between momentum and mass diffusivities. The insets in Fig. 1 show zoomed views of the basic unit element of each geometry with the finest mesh used in the calculations. In the widest part of the symmetrical channel there are 90 by 90 computational cells in the x and y directions respectively, whereas in the narrow channel there are 30 by 30 cells. Therefore, this geometry has a total of 88,200 control volumes, with uniform sizes of $\delta x = \delta y = 2.78\ \mu m$ corresponding to a non-dimensional cell size of $\delta x/2d = 16.66 \times 10^{-3}$.

For the asymmetrical geometry, in the widest part of the channel there are 20 by 60 computational cells in the x and y directions, respectively, whereas in the narrow channel there are 20 by 30 cells. Therefore, this geometry has a total of 54,200 control volumes of uniform size $\delta x = \delta y = 4.17 \mu m$ corresponding to $\delta x/2d = 16.68 \times 10^{-3}$ i.e., the meshes used in both geometries are necessarily different, but have the same degree of refinement.

These are still preliminary calculations and the degree of mesh refinement is not very high, but nevertheless they are of sufficient quality for the results to be of acceptable quality and not too dependent on the mesh. This is well shown in the following two sets of figures for the symmetric (Fig. 2) and asymmetric (Fig. 3) geometries. In both cases we compare results in the mesh used in subsequent calculations, here called fine mesh, with those in a coarse mesh having the following characteristics. In the symmetric geometry the coarse mesh had 72 by 72 uniform cells in the x and y directions in widest part of the channel and 24 by 24 uniform cells in the narrow channel, leading to a total of 66,768 control volumes, with $\delta x = \delta y = 3.47\ \mu m$ corresponding to $\delta x/2d = 20.82 \times 10^{-3}$.

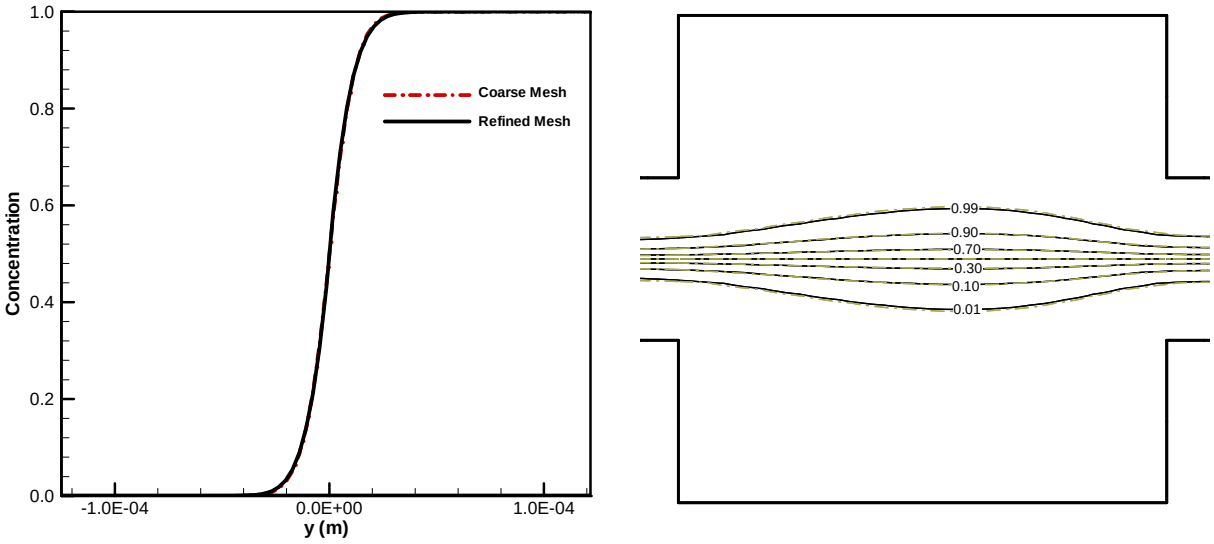

a) b)

Fig. 2 - The effect of mesh refinement on the concentration for the symmetric geometry at *Re*=5, *Pe*= 7.5×10^3: a) Concentration profile across the channel (In the middle of the 3rd expansion block) and b) Comparison between the concentrations contours.

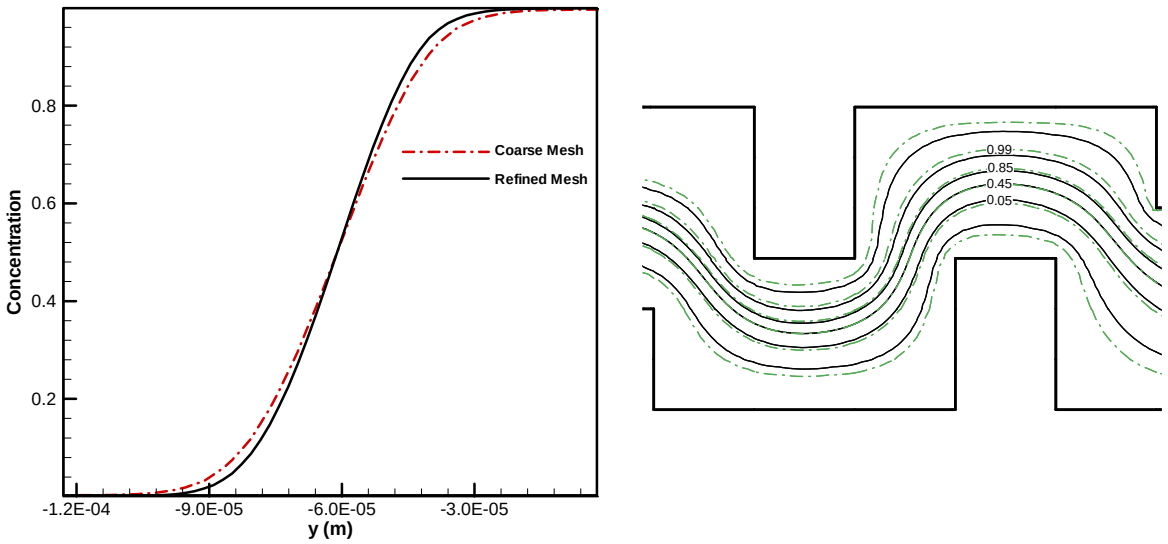

a) b)

Fig. 3 - The effect of mesh refinement on the concentration for the asymmetric geometry at *Re*=5, *Pe*= 5×10^3: a) Concentration profile across the channel (In the middle of the 8th asymmetric obstacle) and b) Comparison between the concentrations contours.

For the asymmetric geometry the comparison between results in the fine and coarse mesh are of similar quality, with near collapse in the center and some difference at the edge of the main jet. The coarse mesh here has the following characteristics: there are 15 by 48 computational cells in the widest part of the channel, in the *x* and *y* directions respectively, and 15 by 24 cells in the narrow channel. Thus, there are a total of 32,070 control volumes of size $\delta y \cong \delta y = 5.21 \mu m$.

4 Results and discussion

In this section the results of the detailed numerical simulations are presented and discussed, starting with the symmetric geometry and followed by the asymmetric channel. Prior to these results it is important to discuss some aspects related to the layout of microgeometries and a few general issues.
The numerical channels are identical to channels that were manufactured for experimental work and it was here important to avoid unnecessarily long geometries, which would be fragile to manipulate and expensive to manufacture. This was achieved by choosing inlets at 90° with the main channel, thus reducing the so-called transition zone and to induce a suitable concentration gradient.
In both geometries, calculations were performed in the range of Reynolds number between 0.05 and 100 and we split the discussion into two separate regimes: $Re < 10$ and $10 < Re < 100$. In our calculations, the fluid is assumed to have a dynamic viscosity of 10^{-3} N.s/m^2 and a density of 10^3 kg/m^3. For the concentration analysis the diffusion coefficient was varied between $D=10^{-7}$ to 10^{-10} m^2/s.
We present the results as contour plots of velocity and of the stream function (streamlines). In addition, in order to understand and to assess the mixing performance, we present contours of *c* and we evaluate the mixing quality at the end of each channel using a mixing index (*Q*), which is defined [13] as:

$$Q = \sqrt{\frac{\sum (C_i - C_m)^2}{N}} \qquad (6)$$

Where $\boldsymbol{C_m}$ is the average concentration at the outlet, for a perfectly mixed condition, $\boldsymbol{C_i}$ is the local concentration at each node of a given cross section of the channel, and *N* is the number of nodes at that cross section. Therefore, the mixing index is equal to 0.5 at the two inlets and becomes equal to 0 when the two fluids are completely mixed.

4.1 Symmetric channels

A detailed investigation was carried out over a wide range of Reynolds numbers, in order to understand the flow behavior, including the visualization of streamlines and velocity contours plots.
The numerical streamlines, obtained at two different Reynolds numbers, are shown in Fig. 4. For a Reynolds number of 5 (Fig. 4a), small recirculations are formed at the far corners downstream of the expansion and upstream of the contraction with the former being larger than the latter. Note that at vanishing Reynolds numbers both recirculations have the same size, but as inertia becomes important the size of the recirculations at the expansion plane increases and those upstream of the contraction plane decrease, eventually disappearing. In each cell having a sudden expansion followed by a sudden contraction, it is possible that the expanding eddy engulfs the contracting eddy before the latter disappears and a single recirculation spans the cell as shown in Fig. 4b) for $Re=50$. Once the recirculation from the expansion plane reaches the contraction plane further increases in the Reynolds number do not change the flow pattern and the size of the recirculation. Therefore, at large *Re* the flow takes place mainly through a central jet whereas the fluid in the recirculation region remains inside closed eddies that mix with the jet fluid only by diffusion.

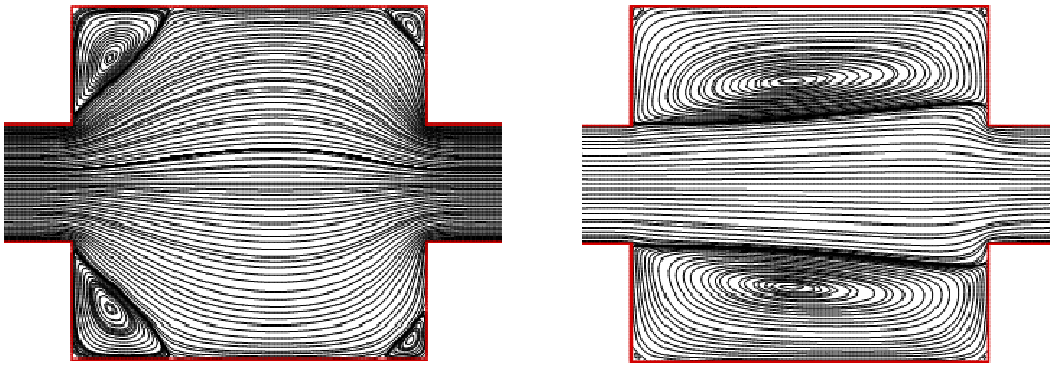

a) b)

Fig. 4 - Streamlines for symmetric geometry at: a) *Re*=5 and b) *Re*=50.

In Figs. 5 and 6, we show contour plots for the lateral (v/V) and axial (u/V) components of the velocity, respectively at different values of *Re*. As explained previously, at the two inlets constant fluid velocities were imposed, which developed very fast into laminar velocity profiles at the inlet channels. These high velocity central jets lead to a concomitant reduction in residence time of fluid that consequently reduces the mixing. It is clear, especially from inspection of Fig. 6a) and 6b) that the jet becomes straighter as the Reynolds number increases.

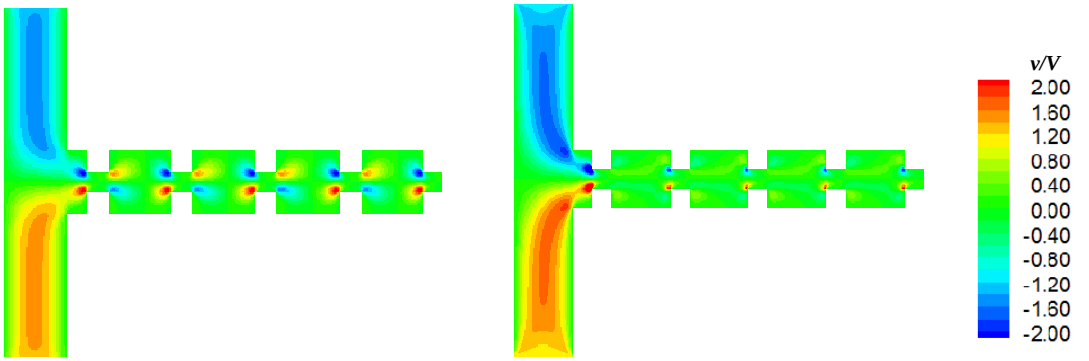

a) b)

Fig. 5 - Transverse velocity contours, v/V for the symmetrical geometry at: a) *Re*=5 and b) *Re*=50.

The contours of v in the inlet channels are consistent with the parabolic velocity profile typical of fully-developed flow.

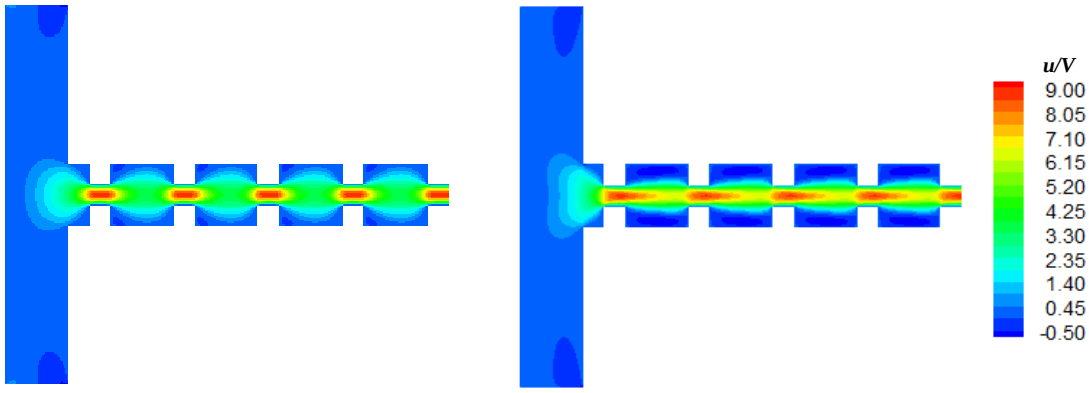

a) b)

Fig. 6 - Axial velocity contour, u/V for the symmetrical geometry at: a) *Re*=5 and b) *Re*=50.

The Péclet and the Reynolds numbers are functions of diffusion coefficients and the flow velocity. A smaller Péclet number results in a more rapid and more uniform mixing. This section presents a parametric study of the effects of Péclet and Reynolds number variation on microfluidic mixing with *Re* varying from 5 to 50 and Péclet number varying from an intermediate value of 7.5×10^2 to 7.5×10^4.
No chemical reaction takes place inside the channel. The concentration of the species is normalized to be one for the inlet in the negative-y direction and zero for the opposite inlet. To track the location of the interface between the two fluids an additional concentration variable (*c*), is transported through the domain by diffusion.
According to Figure 7, we can see that the mixing quality in this geometry is poor in the range $5 \leq Re \leq 50$ for $Pe \geq 7500$. To quantify the mixing quality, the coefficient *Q* of equation (6) was calculated at the exit of the last contraction block, resulting in a value of 0.34 for *Re*=50, and 0.36 for *Re*=5, when the Péclet number was equal to 7.5×10^2. Other results are listed in Table 1. Decreasing the Péclet number from 7.5×10^4 to 7.5×10^3, the mixture was improved marginally from 0.49 to 0.46 since convection still dominates the flow. These two values are nearly identical to 0.5, the value corresponding to no mixing and indicate that this geometry is not suitable for mixing purposes, in spite of the existence of some separated flow regions. The reason for this mixing is simple: mixing is exclusively by diffusion, but mass diffusion is extremely slow by comparison with convection and the fluid has no time to mix within the transit time through the geometry.

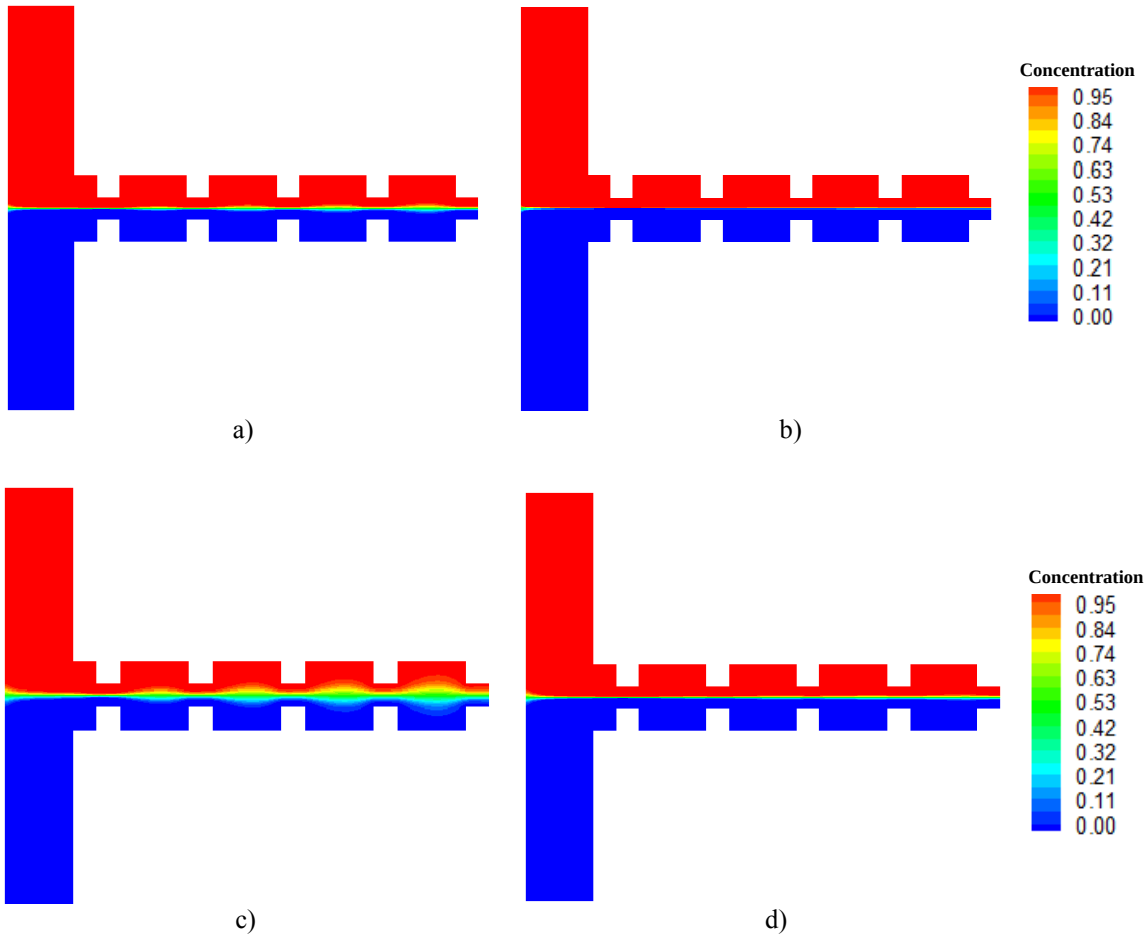

Fig. 7 - Concentration behavior for symmetric geometry at: a) *Re*=5, *Pe*= 7.5×10^3; b) *Re*=50, *Pe*= 7.5×10^4; c) *Re*=5, *Pe*= 7.5×10^2 and d) *Re*=50, *Pe*= 7.5×10^3.

Table 1 - Mixing index for symmetric geometry at the last contraction block.

Péclet numbers	*Re*=5	*Re*=50
Pe=7.5×10^2	0.36	0.34
Pe=7.5×10^3	0.46	0.46
Pe=7.5×10^4	0.49	0.49

4.2 Asymmetric channels

Flow disturbances induced by the presence of obstacles create a meandering flow that may trigger flow instabilities and thus increase mixing. In the present asymmetric channel the geometric disturbances do not generate chaotic advection, because the geometry is two dimensional and the flow remains steady, but nevertheless the flow becomes more complex than in the symmetric case as can be assessed in the streamline plots of Fig. 8. Chaotic advection can only take place in two-dimensional time-dependent and three-dimensional flows [5]. At low Reynolds numbers (Re<10) the fluid meanders and no recirculations are visible except at the far corners and these are very small. Increasing the Reynolds number above 10 leads to the formation of recirculations and the central meandering jet in fact meanders less in some locations as can be observed in Fig. 8b) for Re= 50 and by comparison with the plot of Fig. 8a) for Re= 5.
These features are also clear in the contour plots of the axial velocity component and the trend with increasing Reynolds number is similar to that seen in the symmetric geometry.

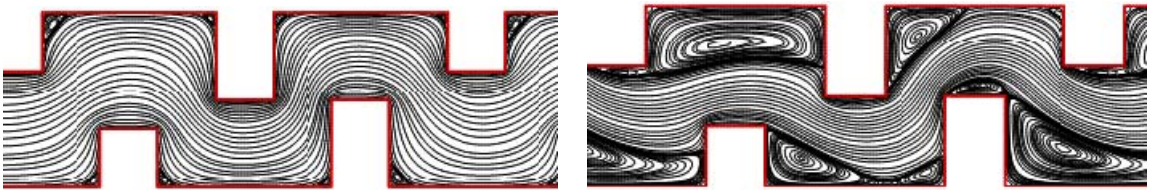

a) b)

Fig. 8 - Streamlines for symmetric geometry, at a) Re=5, b) Re=50.

The meandering flow in the asymmetric geometry increases the path of the fluid particles and consequently their transit time across the channel, offering enhanced opportunity for mixing. A second difference relative to the symmetric geometry is that the cross section of the meandering jet is actually larger than the cross-section of the straight jet by a factor of about 50% since the maximum values of u/V are now about 6 against 9 for the symmetric channel. This means that for identical Reynolds number flows, the fluid particles in the core of the jet, where the large concentration gradient is found, spend at least 50% more time inside the asymmetric channel than in the symmetric one. However, note that the increased time is small and unlikely to produce significant changes when the Péclet number is very high, as was the case in the symmetric flow geometry.
The larger interfacial between mixing fluid streams, provides more chances to fluid molecules to diffuse across each other and improve the mixing of the fluids.
Figs. 9a) and 9b) shows contour plots of scalar concentration for the asymmetric geometry under the same conditions (Pe and Re) of Fig. 7 for the symmetric channel. We observe that mixing is significantly better in the asymmetric geometry. Given the flow description above, we expected a better mixing by a small amount, since the fluid spends more time in this geometry.

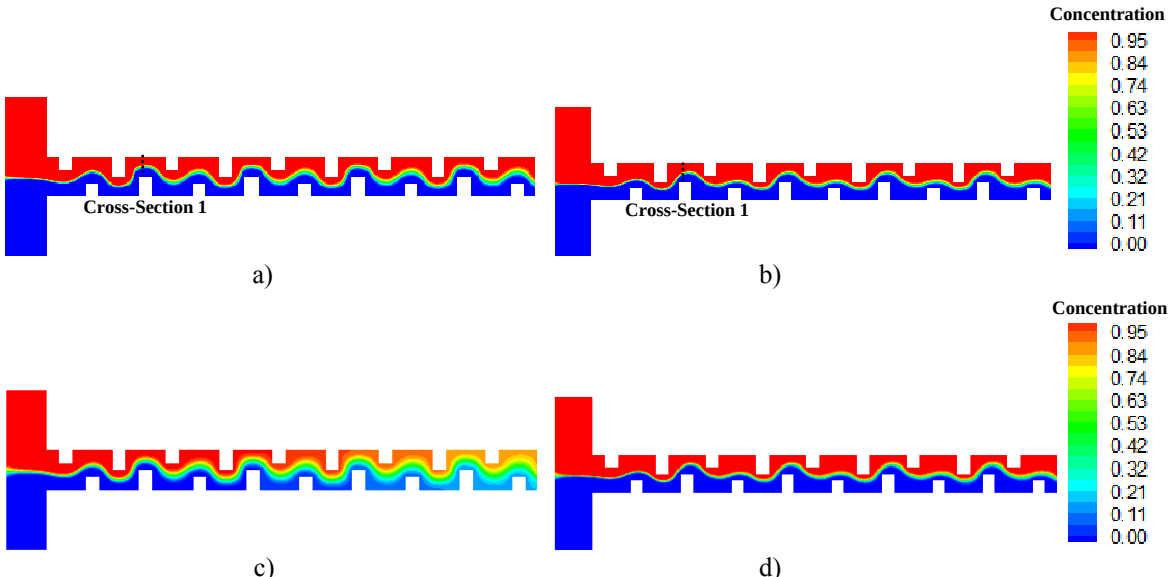

a) b)

c) d)

Fig. 9 - Concentration behavior for symmetric geometry at: a) Re=5, Pe= 5×10^3**;** b) Re=50, Pe= 5×10^4**;** c) Re=5, Pe= 5×10^2 and d) Re=50, Pe= 5×10^3.

The mixing parameter has also been quantified for this asymmetric case at cross section 1 and at the last obstacle (c.f. Fig. 9a) and the results are listed in Table 2. For the flow at Re= 5, parameter Q decreases substantially from 0.49 to 0.42 between the cross-section 1 and the last obstacle, as illustrated in Fig. 9a), indicating a mixing improvement along the channel. A similar behavior is seen for Re=50, with the mixing index decreasing from 0.49 to 0.44 as the fluid flows from cross-section 1 to the last obstacle, respectively, at an identical Péclet number (Pe= 5×10^3). The values of Q at the last obstacle we listed in Table 2 and we see that their values are smaller than in the symmetric geometry, as expected, at similar values of Péclet numbers.
The meandering flow is very often at an inclined angle relative to the orientation of the control volumes, the flow condition that most facilitates numerical diffusion. However, we emphasize that for the solution of the scalar equation we are using the high-resolution scheme CUBISTA of Alves et al [11] which is of third order accuracy.

Table 2 - Mixing index for asymmetric geometry at the last obstacle.

Péclet numbers	Re=5	Re=50
Pe=5×10^2	0.24	0.22
Pe=5×10^3	0.42	0.44
Pe=5×10^4	0.45	0.46

5 Conclusions

A finite volume code was used to study numerically the mixing characteristics of Newtonian fluids flowing inside two T-mixer geometries with different configurations, containing either symmetric or asymmetric constrictions. Since the mass diffusivity was constant, the fluid dynamic problem was decoupled from the mass transfer and both could be solved separately. The Reynolds number was varied between 0.05 and 100 and the Peclet number was varied between 5×10^2 and 5×10^4 for asymmetric geometry and 7.5×10^2 and 7.5×10^4 for the symmetric. For low Reynolds number flow (Re < 5) in the symmetric geometry the strategy of creating a succession of sudden contractions and expansions was not effective to create mixing, which was found to be completely dominated by diffusion and therefore quite slow for the fluid transit times. In contrast, for the asymmetric geometry a meandering flow was created and the mass transfer calculations showed mixing improvement.
The next step of this work will be to extend the investigation to viscoelastic fluids and to try also other geometries, in particular three-dimensional flow geometries.

Acknowledgements

The authors are grateful to FCT for funding this work via project PTDC/EQU-FTT/70727/2006.

References

1. M. Kakuta, F. Bessoth, A. Manz, Microfabricated devices for fluid mixing and their application for chemical synthesis, *Chemical Record*, 1, 395-405, 2001.
2. Z. Wu, N. Nguyen, X. Huang, Non-linear diffusive mixing in microchannels, *Journal of Micromechanics and Microengineering,* 14, 604-11, 2004.
3. N. Trung Nguyen, Z. Wu, Micromixers, *Journal of Micromechanics and Microengineering*, 15, 1-16, 2005.
4. N. Nguyen, S. Werely*, Fundamentals and applications of microfluidics*, Artech House, Boston, 2002.
5. A. D. Stroock, S. Dertinger et al., Chaotic Mixer for Microchannels, *Science,* vol. 295, 647-651, 2002.
6. H. Wang, P. Iovenitti et al., Optimizing layout of obstacles for enhanced mixing in microchannels, *Institute of Physics Publishing*, 11, 662-667, 2002.
7. Gobby, P. Angelli, A.G., Mixing Characteristics of T-type Microfluidic mixers, *Journal of Micromechanics and Microengineering*, 11, 126-132, 2002.

8. M. S. Virk, A. Holdo, S. Kaennakham, Numerical analysis of fluids in T-shape micromixer, *COMSOL users conference, Grenoble*, 2007.
9. S. Hossain, M. A. Ansari, K. Kim, Evaluation of mixing performance of three passive micromixers, *Chemical Engineering Journal*, 150, 492-501, 2009.
10. P. J. Oliveira, F.T. Pinho, Plane contraction flows of upper convected Maxwell and Phan-Thien Tanner fluids as predicted by a finite-volume method, *J. Non-Newtonian Fluid Mech*, 88, 63-88, 1999.
11. M. A. Alves, P. J. Oliveira, F. T. Pinho, A convergent and universally bounded interpolation scheme for the treatment of advection, *International Journal for Numerical Methods in Fluids*, 41, 47-75, 2003.
12. P. J. Oliveira, F.T. Pinho, G.A. Pinto, Numerical simulation of non-linear elastic flows with a general collocated finite-volume method, *J. Non-Newtonian Fluid Mech*., 79, 1-43, 1998.
13. M. Joo-Sung, Y. Kisoo and S. Simon, Modeling for Fluid Mixing in Passive Micromixers Using the Vortex Index, *Journal of the Korean Physical Society*, 48, 902-907, 2006